Scleroderma-specific autoantibodies embedded in immune complexes mediate endothelial damage: an early event in the pathogenesis of systemic sclerosis

Elena Raschi
Istituto Auxologico Italiano Istituto di Ricovero e Cura a Carattere Scientifico
Daniela Privitera
Istituto Auxologico Italiano Istituto di Ricovero e Cura a Carattere Scientifico
Caterina Bodio
Istituto Auxologico Italiano Istituto di Ricovero e Cura a Carattere Scientifico
Paola Adele Lonati
Istituto Auxologico Italiano Istituto di Ricovero e Cura a Carattere Scientifico
Maria Orietta Borghi
Universita degli Studi di Milano Facolta di Medicina e Chirurgia
Francesca Ingegnoli
Universita degli Studi di Milano-Bicocca Scuola di Medicina e Chirurgia
Pier Luigi Meroni
Istituto Auxologico Italiano Istituto di Ricovero e Cura a Carattere Scientifico
Cecilia Beatrice Chighizola (cecilia.chighizola@unimi.it)
University of Milan, Istituto Auxologico Italiano https://orcid.org/0000-0002-3787-9632

Research article

Keywords: Systemic sclerosis, Autoantibodies, Immune complexes, Toll-like Receptors, Endothelial cells, Fibrosis, Inflammation

Posted Date: October 16th, 2020

DOI: https://doi.org/10.21203/rs.3.rs-18870/v2

Version of Record: A version of this preprint was published on November 9th, 2020. See the published version at https://doi.org/10.1186/s13075-020-02360-3.

Abstract

Background: Consistently with their diagnostic and prognostic value, autoantibodies specific for systemic sclerosis (SSc) embedded in immune complexes (ICs) elicited a pro-inflammatory and pro-fibrotic cascade in healthy skin fibroblasts, engaging Toll-like Receptors (TLRs) via their nucleic acid components. The objective of this study was to investigate the pathogenicity of SSc-ICs in endothelial cells.

Methods: ICs were purified from sera of SSc patients bearing different autoantibody specificities (antibodies against DNA topoisomerase I, centromeric proteins, RNA polymerase and Th/To), patients with systemic lupus erythematosus (SLE), primary anti-phospholipid syndrome (PAPS) or healthy controls (NHS) using polyethylen glycol precipitation. Human umbilical vein endothelial cells (HUVECs) were incubated with ICs, positive and negative controls. mRNA levels of *endothelin-1 (et-1)*, *collagenIa1 (colla1)*, *interferon (IFN)-α* and *IFN-β* were investigated by Real-Time PCR; *et-1* and *il-6* mRNA levels were assessed after pre-treatment with bafilomycin. ICAM-1 expression was evaluated by cell-ELISA; secretion of IL-6, IL-8 and transforming growth factor (TGF)-β1 in culture supernatants was measured by ELISA. The expression of Fcg receptors (CD64, CD32 and CD16) was assessed in endothelial cells at FACS analysis. Intracellular signalling pathways culminating with NFkB, p38MAPK, SAPK-JNK and Akt were assessed by Western Blotting. Healthy skin fibroblasts were stimulated with supernatants from HUVEC incubated with ICs, and TGF-b1 secretion, mRNA levels of *colla1* and *matrix metalloproteinase (mmp)-1*, protein expression of . a smooth muscle actin (a-SMA) and IL-6 were evaluated by Western Blotting*; et-1* mRNA levels were assessed in fibroblasts pre-treated with IL-6 and TGF-b inhibitors and stimulated with ATA-ICs.

Results: All SSc stimulated IL-6 secretion; ACA-ICs and anti-Th/To-ICs increased ICAM-1 expression; all SSc-ICs but anti-Th/To-ICs augmented IL-8 levels; all SSc-ICs but ACA and ARA-ICs up-regulated *et-1* and all SSc-ICs but ARA-ICs affected TGF-b1 secretion. *colla1*, *IFN-a* and *IFN-b* mRNA levels were not affected by any SSc-ICs. FcgRII (CD32) and FcgRIII (CD16) were not detectable on HUVECs, while FcgRI (CD64) was minimally expressed. A differential modulation of *tlr* expression was observed: *tlr2*, *tlr3* and *tlr4* were up-regulated by ATA-ICs and ACA-ICs, while anti-Th/To-ICs resulted in *tlr9* up-regulation. Pre-treatment with bafilomycin did not affect the up-regulation of *et-1* and *il-6* induced by ATA-ICs, ACA-ICs and anti-Th/To-ICs; a 23% reduction in both genes was reported for ARA-ICs. All SSc-ICs activated p38MAPK and AKT, all SSc-ICs but ARA-ICs yielded the activation of NFkB; ATA-ICs and ACA-ICs increased the activation rate of both subunits of SAPK-JNK.

When healthy skin fibroblasts were stimulated with supernatants from HUVECs incubated with SSc-ICs, TGF-b1 secretion, *colla1,* a-SMA and IL-6 expression levels were significantly modulated. Pre-treatment

with IL-6 and TGF-b inhibitors prevented *et-1* up-regulation induced by ATA-ICs by 85% and 77% respectively.

Conclusions: These data provide the first demonstration of the pathogenicity of ICs from scleroderma patients with different autoantibodies on the endothelium. Endothelial activation induced by SSc-ICs ultimately led to a pro-fibrotic phenotype in healthy skin fibroblasts.

Background

Systemic sclerosis (SSc) is a chronic systemic autoimmune condition, burdened by the highest mortality among all the rheumatic diseases [1]. The prominent clinical feature of SSc is cutaneous involvement: fibrosis leads to skin tightness, itchiness, loss of skin appendages and subcutaneous fat. It is thus not surprising that the disease was originally named “scleroderma”, from the ancient greek words “scleroV” (tight) and “derma” (skin) [2]. Over time, it has been progressively acknowledged that SSc might be highly polymorphic in terms of clinical presentations. Besides the skin, the fibrotic derangement with deposition of collagen and other components of extra-cellular matrix (ECM) might virtually affect any organ, culminating in tissue dysfunction: most commonly, the gastrointestinal tract, the heart, and the lungs. Other clinical manifestations of SSc acknowledge a vascular aetiology: pulmonary arterial hypertension (PAH), scleroderma renal crisis (SRC) and gastric antral vascular ectasia (GAVE) are underpinned by a fibroproliferative microangiopathy [3]. Given the complexity of the clinical picture, the major challenge in SSc consists in the accurate stratification of the risk of future complications. To date, the most reliable tool to predict the pattern of organ involvement is provided by the fine specificity of SSc-specific autoantibodies [4]. These autoantibodies are generally mutually exclusive and highly specific for SSc, being incorporated in the most recent classification criteria for this condition [5]. The autoantibody reactivity allows patients to be stratified early in disease course, leading to a tailored approach and management [3, 5, 6]. Antibodies against DNA topoisomerase I (ATA) are predictors of the development of interstitial lung disease (ILD) and digital ulcers, but appear to be protective against PAH. Antibodies against centromeric proteins (ACA) predict subcutaneous calcinosis, PAH and gastrointestinal involvement but confer protection against the development of SRC, ILD, synovitis, tendon friction rubs, joint contractures and myopathy. Antibodies directed against RNA polymerase III (ARA) have been linked to severe cutaneous involvement, with flexion contracture of hands and tendon friction rubs. ARA provide one of the strongest risk factors for SRC and GAVE, being protective against ILD and inflammatory myopathy. Antibodies against Th/To (anti-Th/To) correlate with limited cutaneous involvement and severe ILD [4, 7].

The strong association with SSc and the role as prognostic biomarkers suggest the potential pathogenicity of these autoantibodies, similarly to what reported for systemic lupus erythematosus (SLE) [8], anti-phospholipid syndrome (APS) [9], Sjogren’s syndrome [10] and congenital cardiac block [11], inflammatory myopathies [12] and immune-mediated necrotizing myopathies [13]. Evidence of the

pathogenic role of SSc-specific antibodies was raised by our group, with the demonstration that scleroderma-specific autoantibodies bound to their antigens to form immune complexes (ICs) elicit pro-inflammatory and pro-fibrotic effects on healthy skin fibroblasts. According to our previous work, the effects of SSc-ICs on fibroblasts might be mediated by Toll-Like Receptors (TLRs) interacting with the nucleic acid fragments embedded in scleroderma ICs [14].

Fibroblasts are regarded as master players in SSc pathogenesis, being responsible of the ultimate event, namely the excessive deposition of extra cellular matrix (ECM). However, the aetiopathogenesis of such a complex disease is an intricate interplay between many cell types: besides fibroblasts, endothelial cells are key pathogenic effectors [15]. Therefore, the aim of this study was to broaden our previous findings on the pathogenicity of SSc-ICs by assessing the pro-inflammatory and pro-fibrotic effects of scleroderma ICs in healthy endothelial cells.

Materials And Methods

Serum samples.

Serum samples were obtained from twelve patients with SSc fulfilling 2013 ACR/EULAR criteria [5]. All patients had anti-nuclear antibodies (ANA) at indirect immunofluorescence on HEp-2 cells, at a titer greater than 1:160, with staining patterns consistent with the antigenic specificity. Four patients carried ATA, four ACA, two ARA and two anti-Th/To. The remaining autoantibody profile was negative. In all cases, antibody reactivities against scleroderma antigens were confirmed using two different techniques: line blot (“EUROLINE-SSc profile”, Euroimmun, Lubeck, Germany, which includes the following antigens: Ro52, PDGF receptor, Ku, Pm/Scl75, PM-Scl100, Th/To, NOR90, Fibrillarin, RP155, RNA Polymerase III RP11, CENP B, CENP A, and DNA topoisomerase I) and chemiluminescent immunoassays (“QUANTA Flash CTD Screen Plus”, INOVA Diagnostics, San Diego, CA, USA, which detects antibodies against dsDNA, Sm/RNP, Ro52, Ro60, SSB, DNA topoisomerase I, centromere, Mi-2, Ku, Th/To, RNA Polymerase III, Pm/Scl, PCNA, Jo-1, and ribosomal P). The demographic and clinical features of enrolled SSc patients are detailed in **Table 1**. Two SLE patients were recruited; one patient carried anti-Sm, anti-U1 ribonucleoprotein (RNP) and anti-double stranded DNA antibodies, the other harbored anti-Sm [16]. Serum was also obtained from two subjects with primary anti-phospholipid syndrome (PAPS) and positive lupus anticoagulant test, anti-cardiolipin and anti-b2 glycoprotein I IgG antibodies [17]. Four normal healthy subjects (NHS), matched on age and gender to patients, with no autoimmune disease and negative autoantibody profile, were enrolled. Serum samples were stored at -20°C.

Endothelial cell culture.

Human umbilical vein endothelial cells (HUVECs) were isolated from normal term umbilical cord vein by type II collagenase perfusion (Worthington, Lakewood, NJ, USA). HUVEC cell cultures were maintained in complete E199 medium (Flow Labs) supplemented with 20% heat inactivated foetal bovine serum (FBS; PAA Laboratories-GE Healthcare), 1% L-glutamine (MP Biomedicals Inc.), 100 U/ml penicillin-streptomycin (MP Biomedicals) and 250 ng/ml Amphotericin B (MP Biomedicals). Confluent cells were

passaged with a 0.25% trypsin/EDTA (Gibco-Life Technologies) [18]. In all the experiments, a pool of cells from at least three donors were used at the first passage.

Healthy skin fibroblast cell culture.

Dermal fibroblasts were isolated from skin biopsies from two NHS. Under local anesthesia with 1% xylocaine, 5 mm punch skin biopsies were performed in the distal forearm. Samples were minced into small pieces, and digested by collagenase type I (ThermoFisher Scientific Inc, Waltham, MA, USA) for 2 hours at 37°C with 5% CO_2. After a centrifugation at 300g for 10 minutes, pellets were resuspended in 1 ml D-MEM (Gibco-Life Technologies, Groningen, NL) supplemented with 20% Fetal Bovine Serum (FBS, PAA-GE Healthcare, Buckinghamshire, UK), 2 mM glutamine (Sigma-Aldrich), penicillin (100 U/ml)-streptomycin (100 mg/ml) (Sigma-Aldrich) and transferred into a T25 plate (Corning Incorporated, NY, USA). Cultures were maintained at 37°C in 5% CO_2-humidified incubator until confluence. Non-adherent cells and dermal tissue were removed by washing, established fibroblasts were passaged after trypsin/EDTA (ThermoFisher Scientific) release up to the eight passage. Cells were maintained in D-MEM with 10% FBS, 2 mM glutamine, penicillin (100 U/ml)-streptomycin (100 mg/ml) (ThermoFisher Scientific) or incubated overnight in D-MEM with 1% FBS before functional studies. The purity of fibroblast culture was 98% as detected by flow cytometry using a mouse anti-human CD90 and a mouse anti-human CD45 antibodies–PE conjugated (BD Biosciences, San Jose, CA, USA).

Healthy skin fibroblasts were stimulated with supernatants from HUVECs incubated with scleroderma and control ICs for 24 hours. The mRNA levels of collagen *(col)Ia1* and matrix metalloproteinases *(mmp)-1*, the secretion of transforming growth factor (TGF) -b1 and the protein expression levels of a smooth muscle actin (a-SMA) and IL-6 were evaluated. In the latter experiments, fibroblasts were also stimulated with tumour necrosis factor (TNF) -a (10 ng/mL, R&D Systems) and with supernatants from HUVECs incubated with TNF-a for 24 hours as positive controls.

Immune complexes.

ICs were precipitated from NHS' and patients' sera. Briefly, serum samples were mixed with ice-cold 5% polyethylene-glycol (PEG) 6000 (Sigma-Aldrich; Saint Louis, MO, USA)-0.1 M EDTA (Bioscience, Inc, La Jolla, CA, USA) and incubated overnight at 4°C. Samples were diluted three times with 2.5% PEG 6000 in RPMI (Euroclone S.p.A., Pero, Italy), layered on top of 2.5% PEG 6000 supplemented with 5% human serum albumin (Sigma-Aldrich) and centrifuged at 3900 rpm at 4°C for 20 minutes. Pellets were dissolved in D-PBS to initial serum volume and immediately used at 1:2 dilution [19].

Every sample was used in triplicates, each experiment was repeated twice using SSc-ICs isolated from all patients for each autoantibody specificity and control ICs.

The potential endotoxin contamination of IC preparations was ruled out by limulus amoebocyte lysate (LAL) gel-clot test (Pyrosate Kit, Associates of Cape Cod Incorporated, East Falmouth, MA, USA; sensitivity 0.25 EU/ml).

ICAM-1 expression.

Inter-cellular adhesion molecule (ICAM) -1 surface levels were evaluated by home-made cell ELISA, as in previous studies [20]. Confluent EC monolayers were rested in D-MEM with 1% FBS overnight in 96-well plate.

After 24-hour incubation with 100 ml/well of SSc-ICs, PAPS-ICs, SLE-ICs, NHS-ICs, IL-1b (50 U/ml, PeproTech, Rocky Hill, NJ, USA), LPS (1 mg/ml, R&D Systems, Minneapolis, MN, USA) or medium alone, cells were washed twice with HBSS (Sigma-Aldrich), and incubated for 60 minutes at room temperature with 100 ml/well of murine monoclonal IgG specific for human ICAM-1 (CD54, R&D Systems). The antibody was used at a final dilution of 1:500 in HBSS-FBS 2.5%. After two additional washes, cells were incubated for 90 minutes at room temperature with 100 ml of phosphatase-conjugated goat anti-mouse IgG (Cappel, Cochranville, PA, USA). The secondary antibody was used at a dilution of 1:1.000 in HBSS-FBS 10%. After two washes with HBSS, 100 ml of the enzymatic substrate (p-nitrophenylphosphate in 0.05 M Mg-carbonate buffer pH 9.8, Sigma-Aldrich) were added. The optical density (OD) values were evaluated at 405 nm after 30 minutes of incubation by a semiautomatic reader (Titertek Multiskan MCC/340, Titertek Instruments Inc, Pforzheim, Germany).

IL-6, IL-8, and TGF-b1 protein secretion.

IL-6, IL-8 and TGF-b1 release was evaluated in culture supernatants after 24-hour incubation with SSc-ICs, PAPS-ICs, SLE-ICs, NHS-ICs or agonists [IL-1b and LPS] by commercial ELISAs (R&D Systems).

Fcg receptor expression.

The expression of FcgRI (CD64), FcgRII (CD32) and FcgRIII (CD16) was measured on HUVECs by flow cytometry after subtraction of background signals. Briefly, cells were detached by trypsin/EDTA and washed; 200.000 cells per tube were incubated for 20 minutes at 4°C with FITC mouse monoclonal anti-human CD64 (ThermoFisher), FITC mouse monoclonal anti-human CD32 (Beckman Coulter, Brea, CA, USA), FITC mouse monoclonal anti-human CD16 (BD Pharmingen, San Diego, CA, USA) or mouse anti-human isotype control (BD Biosciences, San Jose, CA). Samples were washed again and suspended in 250 µL cold DPBS/1% FCS. 10.000 events were acquired at medium flow rate. A single fluorochrome dot plot strategy was used to identify FcgR positive endothelial cells. In the experiments, control procedures to establish proper calibration and linearity were performed. Analyses were performed using BD FACSLyric cytometer and BD FACSuite software (BD Biosciences).

tlr2, *tlr3*, *tlr4, tlr7, tlr8* and *tlr9,interferon-a,interferon-b*, *endothelin-1, matrix metalloproteinase-1* and *collagenIa1* mRNA expression levels.

tlr2, *tlr3*, *tlr4, tlr7, tlr8*, *tlr9,interferon (ifn)-a*, *ifn-b* and *endothelin (et)-1* mRNA expression levels were evaluated in HUVECs stimulated for 24 hours with SSc-ICs, PAPS-ICs, SLE-ICs, NHS-ICs or agonists (LPS, Poly I:C and ODN CpG [5 mM, InvivoGen, San Diego, CA, USA]). *mmp-1* and *colla1* were evaluated in healthy skin fibroblasts stimulated for 24 hours with supernatants from HUVECs treated with SSc-ICs,

NHS-ICs or recombinant human TGF-b1 (10 ng/ml, PreproTech, Rocky Hill, JN, USA). Total RNA from cells was purified using Trizol Reagent (ThermoFisher Scientific). Amplification Grade DNase I (ThermoFisher Scientific) was used to eliminate residual genomic DNA. A reverse transcription reaction was performed using SuperScript^{TM} First-Strand Synthesis System for RT-PCR (ThermoFisher Scientific). Universal PCR Master Mix No AmpErase UNG (ThermoFisher Scientific) was used for Quantitative RT-PCR, by ABIPRISM 7900 HT Sequence Detection System (ThermoFisher Scientific). Quantification of mRNA expression was performed with TaqMan® Gene Expression Assay (ThermoFisher Scientific) for each target gene. The following TaqMan® Gene Expression assays were used: Hs01872448_s1 (*tlr2),* Hs01551078_m1 (*tlr3*), Hs00152939_m1 (*tlr4*), Hs01933259_s1 (*tlr7*), Hs00152972_m1 (*tlr8*), Hs00370913_s1 (*tlr9*), Hs00855471_g1 (*ifn-a*), Hs01077958_s1 (*ifn-b*), Hs00174961_m1 (*et-1*), Hs00164004_m1 (*colla1*), Hs00899658_m1 (*mmp-1*) and Hs99999905_m1 (*gapdh*). Expression levels of target genes (*tlr2*, *tlr3*, *tlr4, tlr7 tlr8* and *tlr9*, *ifn-a*, *ifn-b*, *et-1, mmp-1* and *cola1*) were determined by the comparative Ct method normalizing the target to the endogenous gene (*gapdh*). Relative values of target to reference were expressed as Fold change (RQ). The optimal time point to evaluate the mRNA levels of *colla1* was set at 24 hours based on a kinetics curve of the mRNA response to stimulation with TGF-b.

IL-6 and a-SMA protein expression and nuclear factor k B, p38 mitogen activated kinase, SAPK-JNK and Akt activation rate.

IL-6 and a-SMA protein expression was evaluated in fibroblasts stimulated for 24 hours with TNF-a and supernatants from HUVECs treated with SSc-ICs, NHS-ICs and TNF-a. The activation rate of nuclear factor k B (NFkB), p38 mitogen activated kinase (p38MAPK), SAPK-JUN N terminal kinase (JNK) and RAC-a serine/threonine protein kinase (Akt) was assessed in HUVECs incubated for 24 hours with SSc-ICs, PAPS-ICs, SLE-ICs, NHS-ICs and IL-1b. Total proteins were isolated using RIPA Lysis Buffer added with Protease and Phosphatase inhibitor cocktail (Sigma-Aldrich). Protein concentration was evaluated using BCA Protein Assay Kit (ThermoFisher Scientific). Proteins were fractionated by NuPAGE BIS-TRIS by 4-12% SDS-polyacrylamide pre-cast gel electrophoresis and transferred to nitrocellulose using iBlot Transfer Stacks Nitrocellulose (ThermoFisher Scientific). Membranes were blocked for 2 hours at room temperature in PBS/0.05% Tween 20 (PT) (Bio-Rad Laboratories, Hercules, CA, USA) containing 5% non-fat milk powder (Mellin, Milan, Italy), and incubated with anti-human IL-6 (Cell Signaling Technology, Danvers, MA, USA), anti-a smooth muscle actin (a-SMA, Sigma-Aldrich), anti-human α-tubulin (Sigma-Aldrich), anti-human nuclear factor k B (NFkB), anti-human phosphorylated NFkB (pNFkB), anti-human p38 mitogen activated kinase (p38MAPK), anti-human phosphorylated p38MAPK (pp38MAPK), anti-human SAPK-JUN N terminal kinase (JNK) or anti-human phosphorylated SAPK-JNK (anti-pSAPK-JNK) antibodies, anti-human RAC-a serine/threonine protein kinase (Akt) or anti-human phosphorylated Akt (anti-pAkt, Cell Signaling Technology, Danvers, MA, USA). After washes, membranes were incubated in PT/5% non-fat milk powder plus HRP-conjugated secondary antibodies (MP Biomedicals, Santa Ana, CA, USA) and developed using ECL Plus Detection System (ThermoFisher Scientific). Signals were detected using radiographic films (Kodak, Rochester, NY, USA). Image J software (LI-COR Biosciences, Lincoln, NE,

US) was used to analyze and quantify gels. Proteins expression levels of IL-6 and a-SMA were normalized to the housekeeping gene, α-tubulin, and expressed as relative protein levels.

An activation kinetics to evaluate the phosphorylation of intracellular mediators in response to different ICs has been performed at different time-points: 0 – 6 – 24 – 36 hours. At 6 hours, the activation rate of all intracellular study mediators was low. In all cases, the highest activation levels were observed at 24 and 36 hours. However, we observed a decrease in cell viability at 36 hours. Therefore, cells were incubated for 24 hours with the different stimuli.

Bafilomycin pre-treatment.

HUVECs were incubated for 2 hours at 37°C with bafilomycin A1 (Millipore, Temecula, CA, USA, 100 nmol) and then treated with SSc-ICs, PAPS-ICs, NHS-ICs and Poly I:C. RT-PCR for *il-6* and *et-1* was then performed.

IL-6 and TGF-b inhibitors.

Fibroblasts were pre-incubated for 30 minutes at 37° C with inhibitors of IL-6 (rat anti-human monoclonal antibody, ThermoFisher Scientific Inc; 2.5 mg/mL) and TGF-b (mouse anti-human monoclonal antibody, R&D Systems; 5 mg/mL). Pre-treated fibroblasts were then stimulated with supernatants from HUVECs incubated with ATA-ICs and with recombinant TGF-b1 as positive control. The mRNA levels of *et-1* were evaluated.

Statistical analysis.

Descriptive statistics was used to calculate mean and standard deviation (SD). Since our data were derived from *in vitro* experiments conducted under high controlled conditions and originated from a high number of cells, ANOVA test was used to compare different experimental conditions, post-hoc comparisons were assessed by Dunnett's test. With regards to not homogeneity of variance assumption, Welch's correction was applied when required. Paired or unpaired t-tests were performed to compare mean values between two groups. All analyses were performed with GraphPad Prism 5.01. P-values <0.05 were considered significant.

The approval of the Institutional Review Board of Istituto G. Pini, Milan, Italy was obtained; all subjects provided written informed consent.

Results

ICAM-1 expression in endothelial cells treated with immune complexes.

ACA-ICs, anti-Th/To-ICs and PAPS-ICs significantly induced ICAM-1 expression on HUVEC monolayers compared to medium; conversely, no increase in ICAM-1 expression was observed with ATA-ICs, ARA-ICs

and SLE-ICs. Both IL-1b and LPS elicited a significant increase in ICAM-1 protein levels compared to medium (**Figure 1A**).

IL-6 and IL-8 secretionin endothelial cells treated with immune complexes.

All SSc-ICs enhanced IL-6 levels compared to medium. Similarly, IL-1b and LPS drove a significant increase in IL-6 with respect to medium. Conversely, HUVECs incubated with PAPS-ICs, SLE-ICs and NHS-ICs exhibited IL-6 levels similar to cells treated with medium alone (**Figure1B**). All SSc-ICs but anti-Th/To-ICs augmented IL-8 levels compared to medium. IL-1b, LPS and SLE-ICs up-regulated IL-8, whereas PAPS-ICs and NHS-ICs did not affect IL-8 levels (**Figure 1C**).

***et-1* and *ifn* mRNA expression in endothelial cells treated with immune complexes.**

ATA-ICs and anti-Th/To-ICs yielded a significant up-regulation of *et-1* levels compared to the medium, as well as LPS and SLE-ICs. Conversely, ACA-ICs, ARA-ICs, PAPS-ICs, NHS-ICs and IL-1b did not exert any effect (**Figure 2A**). Stimulation with IL-1b, LPS, SSc-ICs and control ICs did not result in a significant modulation of mRNA levels of *ifn-a* and *ifn-b* compared to culture medium.

TGF-b1 secretion, *colla1* mRNA expression in endothelial cells treated with immune complexes.

All SSc-ICs but ARA-ICs evoked a significant up-regulation of TGF-b1 secretion compared to medium alone, while NHS-ICs did not exert any effect. Both IL-1b and LPS did not significantly modulate TGF-b1 levels (**Figure 2B**). The mRNA expression of *colla1* was not significantly affected by stimulation with SSc-ICs, control ICs or IL-1b.

Modulation of *et-1* and *il-6* mRNA levelsin endothelial cells treated with bafilomycin and immune complexes.

Pre-treatment with bafilomycin modulated the expression of study mediators in response to stimulation with ARA-ICs. In particular, we observed a 23% reduction of both *et-1* and *il-6* mRNA levels. Bafilomycin did not affect the up-regulation of *et-1* and *il-6* by ATA-ICs, ACA-ICs, anti-Th/To-ICs and control ICs. Conversely, upon stimulation with Poly I:C, a 43% and 58% decrease in the expression of *et-1* and *il-6* respectively was reported after bafilomycin pre-treatment.

Fcg receptor expression in endothelial cells.

At flow-cytometry analysis, FcgRII (CD32) and FcgRIII (CD16) were not detectable on HUVECs (approximately 2%). Minimal expression of FcgRI (CD64) was observed (approximately 9%) (data not shown).

***tlr* mRNA expressionin endothelial cells treated with immune complexes.**

ATA-ICs and ACA-ICs, as well as LPS, drove a significant increase in *tlr2* mRNA as compared to medium. ARA-ICs, anti-Th/To-ICS, PAPS-ICs, SLE-ICs and NHS-ICs did not significantly modulate *tlr2* mRNA (**Figure**

3A). Similarly, ATA-ICs and ACA-ICs, but not ARA-ICs and anti-Th/To-ICs, promoted a significant *tlr3* up-regulation; an increase in *tlr3* mRNA was also observed with Poly I:C and PAPS-ICs. SLE-ICs and NHS-ICs did not affect the mRNA levels of *tlr3* (**Figure 3B**). ATA-ICs and ACA-ICs, as well as LPS, elicited a significant raise in *tlr4* mRNA levels. ARA-ICs and anti-Th/To-ICs, together with PAPS-ICs, SLE-ICs and NHS-ICs, did not affect *tlr4* mRNA levels (**Figure 3C**). *tlr9* expression was significantly modulated by anti-Th/To-ICs, SLE-ICs, LPS and ODN CpG. Conversely, ATA-ICs, ARA-ICs, ACA-ICs, PAPS-ICs and NHS-ICs did not affect *tlr9* mRNA levels (**Figure 3D).** *tlr7* and *tlr8* mRNA could not be detected in HUVECs.

Intra-cellular signaling pathways in endothelial cells treated with immune complexes.

ATA-ICs, ACA-ICs, anti-Th/To-ICs, PAPS-ICs and IL-1b significantly activated NFkB compared to the medium whereas ARA-ICs, SLE-ICs and NHS-ICs did not elicit NFkB phosphorylation (**Figure 4A**). All SSc-ICs, in particular ATA-ICs and anti-Th/To-ICs, induced a significant increased phosphorylation rate of p38MAPK compared to the medium. PAPS-ICs and IL-1b also activated p38MAPK, whereas SLE-ICs and NHS-ICs did not exert any effect on the activation rate of p38MAPK (**Figure 4B**).

ATA-ICs, ACA-ICs, ARA-ICs and IL-1b drove a significant increased phosphorylation rate of p46SAPK-JNK. Anti-Th/To-ICs and NHS-ICs, as well as PAPS-ICs and SLE-ICs, did not exert any effect on the phosphorylation rate of p46SAPK-JNK (**Figure 4C**). ATA-ICs, ACA-ICs, PAPS-ICs and IL-1b yielded a significant increase in p54SAPK-JNK phosphorylation rate. Conversely, ARA-ICs, anti-Th/To-ICs, SLE-ICs and NHS-ICs did not affect the activation rate of p54SAPK-JNK (**Figure 4D**). All SSc-ICs, PAPS-ICs and IL-1b resulted in a significant activation of Akt compared to medium; SLE-ICs and NHS-ICs did not elicit any effect on Akt phosphorylation rate (**Figure 5E**).

TGF-b1 secretion, *colla1*and *mmp-1* mRNA expression in fibroblasts stimulated with supernatants from endothelial cells treated with immune complexes.

Supernatants from HUVECs treated with all SSc-ICs induced a significant increase in TGF-b1 secretion compared to medium in skin fibroblasts, whereas NHS-ICs did not (**Figure 5A**). A significant up-regulation of *colla1* was observed with ATA-ICs and ACA-ICs. ARA-ICs, anti-Th/To-ICs and NHS-ICs did not elicit a significant modulation of *colla1* expression. TGF-b stimulation resulted in a significant raise of *colla1* levels in fibroblasts (**Figure 5B**). SSc-ICs and NHS-ICs as well as TGF-b did not affect *mmp-1* expression in fibroblasts (**Figure 5C**).

a-SMA and IL-6 protein expression in fibroblasts stimulated with supernatants from endothelial cells treated with immune complexes.

Supernatants from HUVECs treated with all SSc-ICs induced a significant increase in a-SMA protein expression compared to medium in skin fibroblasts, whereas NHS-ICs did not. A significant up-regulation of a-SMA was observed even when fibroblasts were treated with TNF-a and with supernatants from HUVECs treated with TNF-a (**Figure 6A**).

Supernatants from HUVECs treated with all SSc-ICs but ACA-ICs significantly up-regulated IL-6 protein expression compared to medium in skin fibroblasts, whereas NHS-ICs did not. A significant up-regulation of IL-6 was observed even when fibroblasts were treated with TNF-a and with supernatants from HUVECs treated with TNF-a (**Figure 6B**).

Pre-treatment with IL-6 and TGF-b inhibitors in fibroblasts stimulated with supernatants from endothelial cells treated with ATA-ICs.

Pre-treatment with both IL-6 and TGF-b inhibitors significantly reduced the mRNA levels of *et-1* in fibroblasts stimulated with supernatants from HUVECs incubated with ATA-ICs compared to not pre-treated cells. In particular, pre-treatment with IL-6 inhibitor resulted in a 85% reduction of *et-1* mRNA expression levels whereas the pre-incubation with TGF-b blocking antibody led to a 77% down-regulation of *et-1* mRNA expression.

Discussion

This in vitro work demonstrates for the first time that scleroderma-specific autoantibodies embedded in ICs induce a pro-inflammatory and pro-fibrotic phenotype even at endothelial level. The hereby presented findings in endothelial cells expand our previous observations on the contribution of SSc-ICs to disease pathogenesis, which were raised in healthy skin fibroblasts. In particular, endothelial incubation with SSc-ICs modulates several molecules involved in the three cardinal scleroderma pathophysiologic processes: vascular dysfunction (ET-1 and IL-8), inflammation (ICAM-1, IL-6) and fibrosis (TGF-b1). Conversely, no modulation of type I IFNs and *colla1* emerges, possibly due to the fact that endothelial cells are not master producers of these mediators. The data presented in this work acquire particular relevance given the fundamental role of endothelial cells in the pathogenesis of SSc. Indeed, endothelial damage is regarded as the very first event in disease course, as suggested by the evidence that Raynaud's phenomenon is almost invariably the presenting clinical manifestation in scleroderma [3]. Once activated, endothelial cells contribute to disease pathogenesis mediating the fibroproliferative vasculopathy characteristic of SSc: the unbalanced production of vasoactive mediators results in vasoconstriction; the increased expression of adhesion molecules by damaged endothelial surface promotes leukocyte trans-endothelial migration, activation and accumulation; endothelial cells transdifferentiate into myofibroblasts gaining mesenchymal cell markers. The above-cited events culminate in intima and media proliferation and vessel occlusion ultimately leading to tissue hypoxia, which further promotes cell injury and fibroblast activation [14, 21]. Several potential insults to the endothelium, for instances viral infections, cold exposure or antibodies against endothelial cells, have been proposed as the initial trigger in SSc aetiopathogenesis, without conclusive results. Our data were raised using healthy endothelial cells, thus suggesting that scleroderma-specific antibodies embedded in ICs might contribute to endothelial damage early on disease course. As a support, positivity for scleroderma antibodies and microvasculopathy signs detected by capillaroscopy are consistently identified as the main predictors of evolution into SSc among patients with Raynaud's phenomenon [22]. The damage of endothelial cells induced by SSc-ICs might even precede fibroblast activation. Indeed, our data provide evidence for a

direct interaction between endothelial cells and fibroblasts: upon stimulation with medium from endothelial cell culture treated with SSc-ICs, fibroblasts synthetize higher amount of *colla1*, *tgf-b1,*a-SMA and IL-6. In agreement with previous studies [23-26], these findings strongly suggest that endothelial cells can impact the function of fibroblasts inducing a pro-fibrotic phenotype, and that such effect on fibroblasts might be mediated by both IL-6 and TGF-b synthetized by endothelial cells in response to SSc-IC stimulation, as documented by the high inhibition rates in *et-1* mRNA levels.

The potential pathogenic relevance of antibodies in scleroderma is also suggested by the accumulation of B lymphocytes at sites of diseases, such as around small vessels in affected skin and in the alveolar interstitium in patients with lung involvement. In SSc, autoreactive B cells, which display high affinity for the antigens, escape censure due to defective B lymphocyte selection and regulation, with increased production of IL-6 and IL-8 and decreased synthesis of IL-10 [27]. Further support comes from the evidence of the effectiveness of anti-B cell therapeutic approach: in vivo, the inhibition of CD19 has been shown not only to abrogate autoantibody production but also to ameliorate skin fibrosis; SSc patients, particularly those ATA-positive, benefit of rituximab treatment [28]. The postulate of the pathogenic relevance of functional autoantibodies in SSc pathogenesis has always been appealing for the scleroderma research community, possibly due to the deleterious effects on cells of treatment with sera from patients [29]. Back in 1970s, anti-endothelial antibodies were reported in 30% of SSc patients [30]; in early 2000, the attention shifted to anti-fibroblasts antibodies [31]. Even recently, the research efforts have been focused on additional newly discovered functional autoantibodies reacting against cell surface receptors. This is the case of antibodies against angiotensin II type I receptor (AT1R), endothelin-1 type A receptor (ETAR) and platelet-derived growth factor receptor (PDGFRa) [32]. Support to the pathogenic potential of these functional autoantibodies has been raised both in vitro and in vivo, being however suggestive of a cell-characteristic activation of pathogenic pathways that might account for specific disease manifestations: vascular damage for anti-AT1R and anti-ETAR, fibrosis for anti-PDGFRa antibodies. In addition, these autoantibodies can be detected in a minority of patients' sera and display a much lower specificity compared to SSc-specific antibodies [32]. Our previous work documenting the pathogenicity of SSc-ICs on skin fibroblasts has energized the research on the functional role of SSc-specific autoantibodies. In particular, it has been very recently documented that sera containing ATA and ACA as well as polyclonal IgG antibodies targeting DNA topoisomerase I and centromeric protein B affect the viability and apoptosis rate of healthy skin fibroblasts. The same treatments up-regulated pro-fibrotic molecules as a-SMA, colla1 and transgelin, assessed both as mRNA expression and as protein levels at immunochemistry [33]. To overcome criticisms advocating the nuclear localization of both antigens, the authors claimed that, according to previous studies, DNA topoisomerase I and centromeric protein B can be released from damaged endothelial cells [34, 35]. Our model bypasses the issue of the nuclear localization of antigens since it envisages the interaction of SSc-ICs with target cells to be mediated by nucleic acids embedded in SSc-ICs. Indeed, scleroderma-specific antibodies are directed against a limited set of autoantigens, comprising DNA or RNA or acid nucleic-binding proteins. In our previous work, we have raised evidence for a significant enrichment in nucleic acids of SSc-ICs, which has been recently confirmed by an independent group [36]. These fragments might be exogenous or endogenous in nature,

originating from microbes or self-cells. Interestingly, neutrophil elastase-expressing cells (granulocytes and activated macrophages), all extensively found to infiltrate scleroderma skin, have been recently identified as the main source of self-DNA [36].

According to the present data as well as to our previous study, SSc-ICs might signal in target cells through the interaction of nucleic acids with TLRs. The present work suggests that TLRs mediating cell response to SSc-ICs reside in the cell membrane and not in intra-cellular compartments. Indeed, to characterize the cell localization of TLRs interacting with SSc-ICs, endothelial cells have been pre-incubated with bafilomycin, an inhibitor of the vacuolar-type H+ -ATPase, which prevents the activation of intra-cellular TLRs by interfering with endosomal acidification. We evince that pre-treatment with bafilomycin does not affect at any rate the up-regulation of *il-6* and *et-1* induced by ATA-ICs, ACA-ICs and anti-Th/To. Conversely, a partial modulation of both genes has been observed upon treatment with ARA-ICs. The negligible involvement of endosomal TLR3 and TLR9 in endothelial cell response to SSc-ICs is in agreement with the lack of expression of FcgRs in HUVECs. In dendritic cells and B lymphocytes, SSc autoantibodies were previously shown to be internalized via FcγRs [37]; however, this hypothesis cannot be translated to the endothelium. Indeed, in agreement with other authors, we detect a minimal expression of CD64 while CD32 and CD16 were not detectable [38-40]. Since CD32 displays a high affinity for IgG ICs and is deputed not only to IC uptake but also to intracellular signal transduction, these data suggest that FcgRs do not mediate endothelial cell response to SSc-ICs.

In fibroblasts, stimulation with ICs culminated in the up-regulation of *tlr2*, *tlr3*, *tlr4* and, to a lower extent, of *tlr9* [13]. In the present work, we observe some differences in TLRs modulation in endothelial cells compared to previous data on fibroblasts, suggesting a cell-specific response to treatment with SSc-ICs. Indeed, ATA-ICs and ACA-ICs engage *tlr2*, *tlr3* and *tlr4*, whereas *tlr9* is recruited upon anti-Th/To-ICs. This hypothesis might be novel for SSc, but has been accepted long ago in other systemic autoimmune diseases. It has been indeed demonstrated, both in in vitro and in vivo studies, that DNA- and RNA-containing ICs from SLE patients stimulate plasmacytoid dendritic cells and B cells to secrete IFN-a through TLR9 and TLR7 via the nucleic acid residues [41-45].

In addition, an increasing burden of evidence points towards a prominent and deleterious role in SSc aetiopathogenesis of chronically activated TLRs. There are solid and growing data in support of TLR involvement in SSc: ex vivo data document overexpression of TLRs in lesional tissues from patients; in vitro experiments highlight the overexpression of pro-fibrotic markers upon TLR activation; in vivo studies in different animal models evince the role of TLRs in mediating tissue fibrosis; genetic studies reveal the association of SSc with polymorphisms in *tlr* genes [46]. In addition, SSc patients display increased levels of endogenous ligands of TLR2 (serum amyloid A and S100A7), TLR4 (tenascin C, fibronectin, high mobility group protein B1 [HMGB1] and heat- shock protein 90). Most recently, ICs composed of DNA and CXCL4 (chemokine (C-X-C motif) ligand 4), a cytokine overexpressed in SSc skin, have been identified as novel TLR ligands in SSc, amplifying TLR9 activation and IFN-a production in plasmacytoid dendritic cells [36].

The cell-specificity of the response to SSc-ICs is further suggested by the differential pattern of activation of intra-cellular mediators in endothelial cells as compared to fibroblasts. At endothelial level, ATA-ICs and ACA-ICs engage NFkB, p38MAPK, p46SAPK-JNK, p54SAPK-JNK and Akt. Conversely, a selective activation is registered for ARA-ICs and anti-Th/To-ICs: the first results in the recruitment of p38MAPK, p46SAPK-JNK and Akt, while the latter promotes the activation of p38MAPK and Akt. As expected, stimulation with PAPS-ICs yields the activation of NFkB, p38MAPK, p54SAPK-JNK and Akt whereas SLE-ICs do not affect the activation rate of any intracellular mediator. Such a striking difference might be explained by aetiopathogenic features of the two diseases. Even though in both conditions autoantibodies have been shown to exert not only a diagnostic but also a pathogenic role, aPL display a particular tropism for the endothelium, which provides their main cellular target [47]. Furthermore, in the present work we confirm our previous finding that ICs from SLE and PAPS patients elicit a differential modulation of study mediators compared to SSc-ICs [13], without affecting molecules directly involved in fibrogenesis such as TGF-b1.

SSc-ICs might contribute to scleroderma aetiopathogenesis being responsible of chronic and aberrant activation of TLRs on several cells involved in SSc. Thus, our hypothesis envisages a direct interaction of ICs with TLRs and does not postulate a type III hypersensitivity mechanism, in which small-sized ICs are ineffectively cleared from circulation, deposit in tissues where activate complement leading to a prominent inflammatory response [48]. Indeed, histological examination of scleroderma skin samples reveals lymphocytic and plasma cell infiltrate in perivascular mid-lower dermis, subcutis, subcutaneous fat but Ig staining is typically negative, there is no complement deposition in tissues and serum complement is not consumed [49].

Our data document a characteristic pattern of modulation of cell functionality for each SSc-IC preparation; thus, it would be surely intriguing to hypothesize that scleroderma-associated antigenic specificities might account for the clinical phenotype we observe in patients with a given autoantibody profile. Indeed, the stimulation of both HUVECs and, in turn, of fibroblasts with ATA-ICs results in a marked pro-inflammatory and pro-fibrotic phenotype, a finding that fits well with clinical features of patients carrying ATA. Similarly, ACA-ICs elicit a strong response in HUVECs, consistently with the prevalent vascular involvement that characterizes clinical presentation in patients. Even though our work clearly supports the pathogenic potential of SSc-ICs in both endothelial cells and fibroblasts, we still believe that definitive conclusion on the differential pathogenic potential of SSc-ICs should be drawn cautiously. Indeed, clinical manifestations arise from a close interplay between several cells in a tissue-specific milieu; our in vitro model might be over simplistic, not allowing to adequately reproduce the complexity of scleroderma pathogenesis. Such partial insight into disease aetiopathogenesis provides one of the limitations that flaw our study. To overcome this critical issue, we are implementing a dynamic in vitro model that envisages multiple bioreactors for 3D cell cultures interconnected by a dynamic flow in order to mimic the cell crosstalk that characterizes SSc pathogenesis in humans [50]. Another major limitation of this study relates to the scarce number of samples for each autoantibody specificity; unfortunately, the recruitment of a broader cohort of patients is prevented by the relative rarity of certain antibodies (e.g., ARA and anti-Th/To) in the Italian SSc population [51]. We acknowledge that even the

number of disease controls is low, due to the technical requirement of fresh PEG preparations for in vitro cellular studies. Despite the limited number of samples, the robustness of the conclusions presented in this study, which provides the proof-of-concept of IC deleterious effects on the endothelium, ispreserved.

Conclusion

As a whole, the present work provides novel insights into the pathogenicity of SSc-ICs, yielding a demonstration of the deleterious effects of preparations containing scleroderma autoantibodies on the endothelium. SSc-ICs might be located at a cross-road in scleroderma pathogenesis: future studies should focus on how ICs contribute to the activation of several cells involved in scleroderma pathogenesis. Besides fibroblasts and endothelial cells, SSc-ICs might interact with several other cellular players involved in scleroderma pathogenesis: adipocytes, T cells, macrophages, and plasmacytoid dendritic cells. Insights into SSc-IC pathogenicity might have therapeutic implications, identifying TLRs as candidate pharmacological targets in the initiation phase of the disease, before the onset of overt fibrosis. TLR signaling can be disrupted in multiple ways: blocking TLRs with an antibody, enhancing negative regulators of TLR signaling and/or modifying the epigenetic regulators of TLR signaling. In vivo data have already been raised, since TLR4 and TLR9 antagonists prevented and reversed organ fibrosis in distinct preclinical disease models, highlighting the potential therapeutic benefit of selectively blocking TLR4 activity [46, 52, 53]. Hydroxychloroquine, an anti-malarial whose TLR modulating properties are well established, has been recently shown to ameliorate serum markers of endothelial injury [54]. This future might not be so far away: monospecific TLR7 and TLR9 antagonists are currently under investigation for the treatment of dermatomyositis and plaque psoriasis [52].

Declarations

Ethics approval and consent to participate: This study was approved by the ethical Committee “Milano Area B”, opinion number 426, date July 8th 2014. All patients provided written informed consent to participate.

Consent to publication: All authors consent to the publication of the manuscript.

Availability of data and materials: The datasets supporting the conclusions of this article can be made available upon request.

Competing interests: The authors declare no competing interests.

Funding: This work was supported by Ricerca Corrente 2019, IRCCS Istituto Auxologico Italiano to PLM and Progetto Azione A Giovani Ricercatori, Department of Clinical Sciences and Community Health, University of Milan to CBC.

Authors’ contributions: ER, CBC, PLM and MOB designed the experiments and wrote the manuscript; CBC, FI and PLM were responsible for patients’ enrollment and follow-up; ER, DP and PAL performed the in

vitro experiments; ER, CBC and DP ran the statistical analysis of the data. All authors reviewed and approved the final version of the manuscript.

Acknowledgements: None.

Abbreviations

SSc: systemic sclerosis

ECM: extra-cellular matrix

PAH: pulmonary arterial hypertension

SRC: scleroderma renal crisis

GAVE: gastric antral vascular ectasia

ATA: anti-DNA topoisomerase I antibodies

ILD: interstitial lung disease

ACA: anti-centromeric proteins antibodies

ARA: anti-RNA polymerase III antibodies

anti-Th/To: anti-Th/To antibodies

SLE: systemic lupus erythematosus

PAPS: primary anti-phospholipid syndrome

ICs: immune complexes

ANA: anti-nuclear antibodies

RNP: ribonucleoprotein

NHS: normal healthy subjects

HUVECs: human umbilical vein endothelial cells

FBS: fetal bovine serum

colla1: collagenIa1

MMP: matrix metalloproteinase

TGF: transforming growth factor

SMA: smooth muscle actin

PEG: polyethylene-glycol

RPMI: Roswell Park memorial Institute

ICAM-1: inter-cellular adhesion molecule

OD: optical density

LAL: limulus amoebocyte lysate

ELISA: enzyme-linked immunosorbent assay

HBSS: Hank's balanced salt solution

IL: interleukin

IFN: interferon

et-1: endothelin-1

NFkB: nuclear factor k B

pNFkB: phosphorylated nuclear factor k B

p38MAPK: p38 mitogen activated kinase

pp38MAPK: phosphorylated p38MAPK

JNK: JUN N terminal kinase

AKT: RAC-a serine/threonine protein kinase

P/T: PBS/0.05% Tween 20

SD: standard deviation

AT1R: angiotensin II type I receptor

ETAR: endothelin-1 type A receptor

PDGFR: platelet-derived growth factor receptor

DAMPs: damage-associated molecular patterns

HMGB1: high mobility group protein B1

FcgR: Fcg receptor

CXCL4: chemokine (C-X-C motif) ligand 4

References

1. Tyndall AJ, Bannert B, Vonk M, Airò P, Cozzi F, Carreira PE, et al. Causes and risk factors for death in systemic sclerosis: a study from the EULAR Scleroderma Trials and Research (EUSTAR) database. Ann Rheum Dis 2010;69: 1809–15.
2. Rodnan GP, Benedek TG. An historical account of the study of progressive systemic sclerosis (diffuse scleroderma). Ann Intern Med. 1962;57:305-19.
3. Denton CP, Khanna D. Systemic sclerosis. Lancet. 2017;390:1685–99.
4. Nihtyanova SI, Denton CP. Autoantibodies as predictive tools in systemic sclerosis. Nat Rev Rheumatol. 2010;6:112–6.
5. van den Hoogen F, Khanna D, Fransen J, Johnson SR, Baron M, Tyndall A, et al. 2013 classification criteria for systemic sclerosis: an American College of Rheumatology/European League Against Rheumatism collaborative initiative. Ann Rheum Dis. 2013;72:1747–55.
6. Nihtyanova SI, Sari A, Harvey JC, Leslie A, Derrett-Smith EC, Fonseca C, Ong VH, Denton CP. Using autoantibodies and cutaneous subset to develop outcome-based disease classification in systemic sclerosis. Arthritis Rheumatol. 2020;72(3):465-476.
7. Hamaguchi Y. Autoantibody profiles in systemic sclerosis: predictive value for clinical evaluation and prognosis. J Dermatol. 2010;37(1):42-53.
8. Choi MY, Fritzler MJ. Autoantibodies in SLE: prediction and the p value matrix. Lupus. 2019;28(11):1285-1293.
9. Chighizola CB, Raschi E, Borghi MO, Meroni PL. Update on the pathogenesis and treatment of the antiphospholipid syndrome. Curr Opin Rheumatol. 2015;27(5):476-82.
10. Nocturne G, Mariette X. Advances in understanding the pathogenesis of primary Sjögren's syndrome. Nat Rev Rheumatol. 2013;9(9):544-56.
11. Ambrosi A, Wahren-Herlenius M. Congenital heart block: evidence for a pathogenic role of maternal autoantibodies. Arthritis Res Ther. 2012;14(2):208.
12. Katsumata Y, Ridgway WM, Oriss T, Gu X, Chin D, Wu Y, et al. Species-specific immune responses generated by histidyl-tRNA synthetase immunization are associated with muscle and lung inflammation. J Autoimmun. 2007;29(2-3):174-86.
13. Bergua C, Chiavelli H, Allenbach Y, Arouche-Delaperche L, Arnoult C, Bourdenet G, et al. In vivo pathogenicity of IgG from patients with anti-SRP or anti-HMGCR autoantibodies in immune-mediated necrotising myopathy. Ann Rheum Dis. 2019;78(1):131-139.

14. Raschi E, Chighizola CB, Cesana L, Privitera D, Ingegnoli F, Mastaglio C, et al. Immune complexes containing scleroderma-specific autoantibodies induce a profibrotic and proinflammatory phenotype in skin fibroblasts. Arthritis Res Ther. 2018;20(1):187.
15. Distler JHW, Györfi AH, Ramanujam M, Whitfield ML, Königshoff M, Lafyatis R. Shared and distinct mechanisms of fibrosis. Nat Rev Rheumatol. 2019;15(12):705-730.
16. Hochberg MC. Updating the American College of Rheumatology revised criteria for the classification of systemic lupus erythematosus. Arthritis Rheum. 1997;40:1725.
17. Miyakis S, Lockshin MD, Atsumi T, Branch DW, Brey RL, Cervera R, et al. International consensus statement on an update of the classification criteria for definite antiphospholipid syndrome (APS). J Thromb Haemost. 2006;4:295–306.
18. Crampton SP, Davis J, Hughes CC. Isolation of human umbilical vein endothelial cells (HUVEC). J Vis Exp. 2007;(3):183
19. Pontes-de-Carvalho LC, Lannes-Vieira J, Giovanni-de-Simone S, Galvão-Castro B. A protein A-binding, polyethylene glycol precipitation-based immunoradiometric assay. Application to the detection of immune complexes and C3 in human sera and of private antigens in cross-reacting parasite extracts. J Immunol Methods. 1986;89:27–35.
20. Del Papa N, Guidali L, Sala A, Buccellati C, Khamashta MA, Ichikawa K, et al. Endothelial cells as target for antiphospholipid antibodies. Human polyclonal and monoclonal anti-beta 2-glycoprotein I antibodies react in vitro with endothelial cells through adherent beta 2-glycoprotein I and induce endothelial activation. Arthritis Rheum. 1997;40:551–61.
21. Mostmans Y, Cutolo M, Giddelo C, Decuman S, Melsens K, Declercq H, et al. The role of endothelial cells in the vasculopathy of systemic sclerosis: A systematic review. Autoimmun Rev. 2017;16(8):774-786.
22. Koenig M, Joyal F, Fritzler MJ, Roussin A, Abrahamowicz M, Boire G, et al. Autoantibodies and microvascular damage are independent predictive factors for the progression of Raynaud's phenomenon to systemic sclerosis: a twenty-year prospective study of 586 patients, with validation of proposed criteria for early systemic sclerosis. Arthritis Rheum. 2008;58(12):3902-12.
23. Denton CP, Xu S, Black CM, Pearson JD. Scleroderma fibroblasts show increased responsiveness to endothelial cell-derived IL-1 and bFGF. J Invest Dermatol. 1997;108(3):269-74.
24. Raymond MA, Vigneault N, Luyckx V, Hébert MJ. Paracrine repercussions of preconditioning on angiogenesis and apoptosis of endothelial cells. Biochem Biophys Res Commun. 2002;291(2):261-9.
25. Laplante P, Raymond MA, Gagnon G, Vigneault N, Sasseville AM, Langelier Y, et al. Novel fibrogenic pathways are activated in response to endothelial apoptosis: implications in the pathophysiology of systemic sclerosis. J Immunol. 2005;174(9):5740-9
26. Serratì S, Chillà A, Laurenzana A, Margheri F, Giannoni E, Magnelli L, et al. Systemic sclerosis endothelial cells recruit and activate dermal fibroblasts by induction of a connective tissue growth factor (CCN2)/transforming growth factor β-dependent mesenchymal-to-mesenchymal transition. Arthritis Rheum. 2013;65(1):258-69.

27. Taher TE, Ong VH, Bystrom J, Hillion S, Simon Q, Denton CP, et al. Association of defective regulation of autoreactive interleukin-6-producing transitional B lymphocytes with disease in patients with systemic sclerosis. Arthritis Rheumatol. 2018;70(3):450-461.
28. Thiebaut M, Launay D, Rivière S, Mahévas T, Bellakhal S, Hachulla E, et al. Efficacy and safety of rituximab in systemic sclerosis: French retrospective study and literature review. Autoimmun Rev. 2018;17(6):582-587.
29. Kim D, Peck A, Santer D, Patole P, Schwartz SM, Molitor JA, et al. Induction of interferon-alpha by scleroderma sera containing autoantibodies to topoisomerase I: association of higher interferon-alpha activity with lung fibrosis. Arthritis Rheum. 2008;58:2163–73.
30. Rosenbaum J, Pottinger BE, Woo P, Black CM, Loizou S, Byron MA, et al. Measurement and characterisation of circulating anti-endothelial cell IgG in connective tissue diseases. Clin Exp Immunol. 1988;72(3):450-6.
31. Ronda N, Gatti R, Giacosa R, Raschi E, Testoni C, Meroni PL, et al. Antifibroblast antibodies from systemic sclerosis patients are internalized by fibroblasts via a caveolin-linked pathway. Arthritis Rheum. 2002;46(6):1595-601.
32. Moroncini G, Svegliati Baroni S, Gabrielli A. Agonistic antibodies in systemic sclerosis. Immunol Lett. 2018;195:83-87.
33. Corallo C, Cheleschi S, Cutolo M, Soldano S, Fioravanti A, Volpi N, et al. Antibodies against specific extractable nuclear antigens (ENAs) as diagnostic and prognostic tools and inducers of a profibrotic phenotype in cultured human skin fibroblasts: are they functional? Arthritis Res Ther. 2019;21(1):152.
34. Oppenheim JJ, Dong HF, Plotz P, Caspi RR, Dykstra M, Pierce S, et al. Autoantigens act as tissue-specific chemoattractants. J Leukoc Biol. 2005;77(6):854-61.
35. Robitaille G, Hénault J, Christin MS, Senécal JL, Raymond Y. The nuclear autoantigen CENP-B displays cytokine-like activities toward vascular smooth muscle cells. Arthritis Rheum. 2007;56(11):3814-26.
36. Lande R, Lee EY, Palazzo R, Marinari B, Pietraforte I, Santos GS, et al. CXCL4 assembles DNA into liquid crystalline complexes to amplify TLR9-mediated interferon-α production in systemic sclerosis. Nat Commun. 2019;10(1):1731.
37. Kim D, Peck A, Santer D, Patole P, Schwartz SM, Molitor JA, et al. Induction of interferon α by scleroderma sera containing autoantibodies to topoisomerase I: Association of higher interferon α activity with lung fibrosis. Arthritis Rheum. 2008;58(7):2163–2173
38. Gröger M, Sarmay G, Fiebiger E, Wolff K, Petzelbauer P. Dermal microvascular endothelial cells express CD32 receptors in vivo and in vitro. J Immunol. 1996;156(4):1549-56.
39. Pan LF, Kreisle RA, Shi YD. Detection of Fcgamma receptors on human endothelial cells stimulated with cytokines tumour necrosis factor-alpha (TNF-alpha) and interferon-gamma (IFN-gamma). Clin Exp Immunol. 1998;112(3):533-8.
40. Liang YJ, Shyu KG, Wang BW, Lai LP. C-reactive protein activates the nuclear factor-kappaB pathway and induces vascular cell adhesion molecule-1 expression through CD32 in human umbilical vein

endothelial cells and aortic endothelial cells. J Mol Cell Cardiol. 2006;40(3):412-20.

41. Vollmer J, Tluk S, Schmitz C, Hamm S, Jurk M, Forsbach A, et al. Immune stimulation mediated by autoantigen binding sites within small nuclear RNAs involves Toll-like receptors 7 and 8. J Exp Med. 2005;202(11):1575-85.
42. Viglianti GA, Lau CM, Hanley TM, Miko BA, Shlomchik MJ, Marshak-Rothstein A. Activation of autoreactive B cells by CpG dsDNA. Immunity. 2003;19(6):837-47.
43. Leadbetter EA, Rifkin IR, Hohlbaum AM, Beaudette BC, Shlomchik MJ, Marshak-Rothstein A. Chromatin-IgG complexes activate B cells by dual engagement of IgM and Toll-like receptors. Nature. 2002;416(6881):603-7.
44. Means TK, Latz E, Hayashi F, Murali MR, Golenbock DT, Luster AD. Human lupus autoantibody-DNA complexes activate DCs through cooperation of CD32 and TLR9. J Clin Invest. 2005;115(2):407-17.
45. Boulé MW, Broughton C, Mackay F, Akira S, Marshak-Rothstein A, Rifkin IR. Toll-like receptor 9-dependent and -independent dendritic cell activation by chromatin-immunoglobulin G complexes. J Exp Med. 2004;199(12):1631-40.
46. O'Reilly S. Toll Like Receptors in systemic sclerosis: An emerging target. Immunol Lett. 2018;195:2-8.
47. Chighizola CB, Raschi E, Borghi MO, Meroni PL. Update on the pathogenesis and treatment of the antiphospholipid syndrome. Curr Opin Rheumatol. 2015;27(5):476-82.
48. Kumar V, Abbas AK, Aster JC. Robbins and Cotran pathologic basis of disease. 9th ed, 2014 - Saunders/Elsevier - Philadelphia, PA.
49. Chimenti MS, Di Stefani A, Conigliaro P, Saggini A, Urbani S, Giunta A, et al. Histopathology of the skin in rheumatic diseases. Reumatismo. 2018;70(3):187-198.
50. Ahluwalia A, Misto A, Vozzi F, Magliaro C, Mattei G, Marescotti MC, et al. Systemic and vascular inflammation in an in-vitro model of central obesity. PLoS One. 2018;13(2):e0192824.
51. Ceribelli A, Cavazzana I, Franceschini F, Airò P, Tincani A, Cattaneo R, et al. Anti-Th/To are common antinucleolar autoantibodies in Italian patients with scleroderma. J Rheumatol. 2010;37:2071–5.
52. Volkmann ER, Varga J. Emerging targets of disease-modifying therapy for systemic sclerosis. Nat Rev Rheumatol. 2019;15(4):208-224.
53. Henderson J, Bhattacharyya S, Varga J, O'Reilly S. Targeting TLRs and the inflammasome in systemic sclerosis. Pharmacol Ther. 2018;192:163-169
54. Basta F, Irace R, Borgia A, Messiniti V, Riccardi A, Valentini G, et al. Hydroxychloroquine significantly reduces serum markers of endothelial injury and NEMO videocapillaroscopy score in systemic sclerosis. Rheumatology (Oxford). 2019;58(7):1303-1305.
55. LeRoy EC, Black C, Fleischmajer R, Jablonska S, Krieg T, Medsger TA Jr, et al. Scleroderma (systemic sclerosis): classification, subsets and pathogenesis. J Rheumatol. 1988;15:202–5.

Table

Table 1. Demographic and clinical data of enrolled SSc patients.

	ATA (n=4)	ACA (n=4)	ARA (n=2)	anti-Th/To (n=2)
ge (years)	51 [44.25-55.25]	51 [43.5-60]	37.5 [31.25-43.75]	41.5 [38.75-44.25]
emales (%)	4 (100%)	4 (100%)	2 (100%)	2 (100%)
isease duration (months)*	31 [29.5-33.5]	30.5 [26-34.5]	28 [25-31]	31.5 [30.25-32.75]
cSSc/lcSSc°	3/1	3/1	2/0	0/2
LD (%)¶	2 (50%)	0	0	1 (50%)
AH (%)§	0	1 (25%)	0	1 (50%)
oint involvement (%)	1 (25%)	0	1 (50%)	0
RC (%)#	0	0	0	0
Muscle involvement (%)$	0	0	0	1 (25%)
evere GI involvement (%)&	0	1 (25%)	0	0
eart involvement (%)£	1 (25%)	0	0	0
igital ulcers (%)	1 (25%)	1 (25%)	0	0
aynaud's phenomenon (%)	4 (100%)	4 (100%)	2 (100%)	1 (50%)
MARDs				
HCQ	1	2	1	1
AZA	0	0	0	1
MTX	2	0	1	0
MMF	1	0	0	0

Continuous variables are expressed as median [interquartile range].

*= from the onset of the first non-Raynaud's phenomenon symptom to study inclusion.

¶= forced vital capacity (FVC) or carbon monoxide diffusing capacity of the lung (DL_{CO}) <55% of predicted or a 15% decline from baseline in FVC or DL_{CO}, with evidence of fibrosis on high-resolution CT.

§= mean pulmonary arterial pressure >25 mmHg at right heart catheterization.

#= new-onset systemic hypertension >150/85 mmHg with a decrease in estimated glomerular filtration rate >30%.

$= objective muscle weakness (score<4 on a 5-point Likert scale) and an elevated total creatine kinase level (>4-fold the upper limit of normal).

[&]= at least 3 episodes of intestinal pseudoobstruction requiring hospitalization or requiring >6 weeks of enteral or parental nutritional support.

[£]= haemodynamically significant arrhythmias, pericardial effusion or congestive heart failure.

°= according to LeRoy [55].

dcSSc= diffuse cutaneous systemic sclerosis; lcSSc= limited cutaneous systemic sclerosis; RP= primary Raynaud's phenomenon; n=number; ACA= antibodies against centromeric proteins; ATA= antibodies against DNA topoisomerase I; ARA= antibodies against RNA polymerase III; anti-Th/To= antibodies against Th/To; ILD= interstitial lung disease; SRC= scleroderma renal crisis; GI= gastrointestinal; DMARDs: disease modifying anti-rheumatic drugs; HCQ: hydroxychloroquine; AZA: azathioprine; MTX: methotrexate; MMF: mycophenolate.

Figures

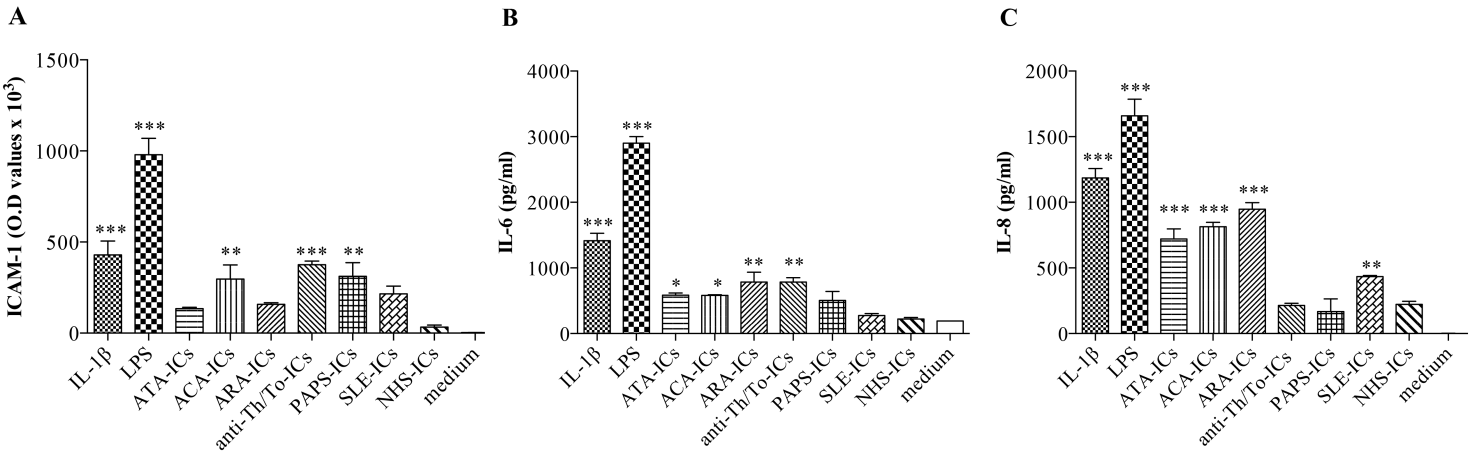

Figure 1

ICAM-1 expression and IL-6 and IL-8 secretion in HUVECs stimulated with SSc-ICs, PAPS-ICs, SLE-ICs or NHS-ICs. Endothelial cells were incubated with SSc-ICs, PAPS-ICs, SLE-ICs or NHS-ICs (1:2 dilution). IL-1□□(50 U/ml) and LPS (1 □g/ml) were used as positive controls. Histograms represent mean ± standard error of the mean (SEM). *p<0.01; **p<0.001; ***p<0.0001 versus medium. (A): ICAM-1 expression (O.D.) [mean±SD]. IL-1□ [429.8±151.9] versus medium [2.75±1.71] (p<0.0001), versus NHS-ICs (p<0.0001). LPS [979.5±180.3] versus medium (p<0.0001), versus NHS-ICs (p<0.0001). ATA-ICs [134±16.27] versus medium (p=N.S.) and versus NHS-ICs [34.25±17.63] (p=N.S.). ACA-ICs [297.3±153.7] versus medium (p<0.001), versus NHS-ICs (p<0.01). ARA-ICs [157.8±17.61] versus medium (p=N.S.), versus NHS-ICs (p=N.S.). Anti-Th/To-ICs [375±42.16] versus medium (p<0.0001), versus NHS-ICs (p<0.0001). PAPS-ICs [311.3±151.7] versus medium (p<0.001), versus NHS-ICs (p<0.001). SLE-ICs [216±84.75] versus medium (p=N.S.), versus NHS-ICs (p=N.S.). NHS-ICs [34.25±17.63] versus medium (p=N.S.). (B): IL-6 expression (pg/mL) [mean±SD]. IL-1□ [1414±161.2] versus medium [191±0.70] (p<0.0001), versus NHS-ICs

(p<0.0001). LPS [2900.5±141.4] versus medium (p<0.0001), versus NHS-ICs (p<0.0001). ATA-ICs [584.5±48.79] versus medium (p<0.01) and versus NHS-ICs [222.5±31.82] (p=N.S.). ACA-ICs [582±15.56] versus medium (p<0.01), versus NHS-ICs (p=N.S). ARA-ICs [785.5±210] versus medium (p<0.001), versus NHS-ICs (p<0.001). Anti-Th/To-ICs [786±90.51] versus medium (p<0.001), versus NHS-ICs (p<0.001). PAPS-ICs [504.5±193] versus medium (p=N.S.), versus NHS-ICs (p=N.S.). SLE-ICs [276.5±40.31] versus medium (p=N.S.), versus NHS-ICs (p=N.S.). NHS-ICs [222.5±31.82] versus medium (p=N.S.). (C): IL-8 expression (pg/mL) [mean±SD]. IL-1β [1186±101.8] versus medium [1.5±0.6] (p<0.0001), versus NHS-ICs (p<0.0001). LPS [1659±178.2] versus medium (p<0.0001), versus NHS-ICs (p<0.0001). ATA-ICs [721.5±108.2] versus medium (p<0.0001) and versus NHS-ICs [222.5±31.82] (p<0.001). ACA-ICs [814.5±47.38] versus medium (p<0.0001), versus NHS-ICs (p<0.0001). ARA-ICs [948±69.3] versus medium (p<0.0001), versus NHS-ICs (p<0.0001). Anti-Th/To-ICs [214±22.63] versus medium (p=N.S), versus NHS-ICs (p=N.S.). PAPS-ICs [167±137.2] versus medium (p=N.S.), versus NHS-ICs (p=N.S.). SLE-ICs [434±11.31] versus medium (p<0.001), versus NHS-ICs (p=N.S.). NHS-ICs [218.2±28.51] versus medium (p=N.S.).

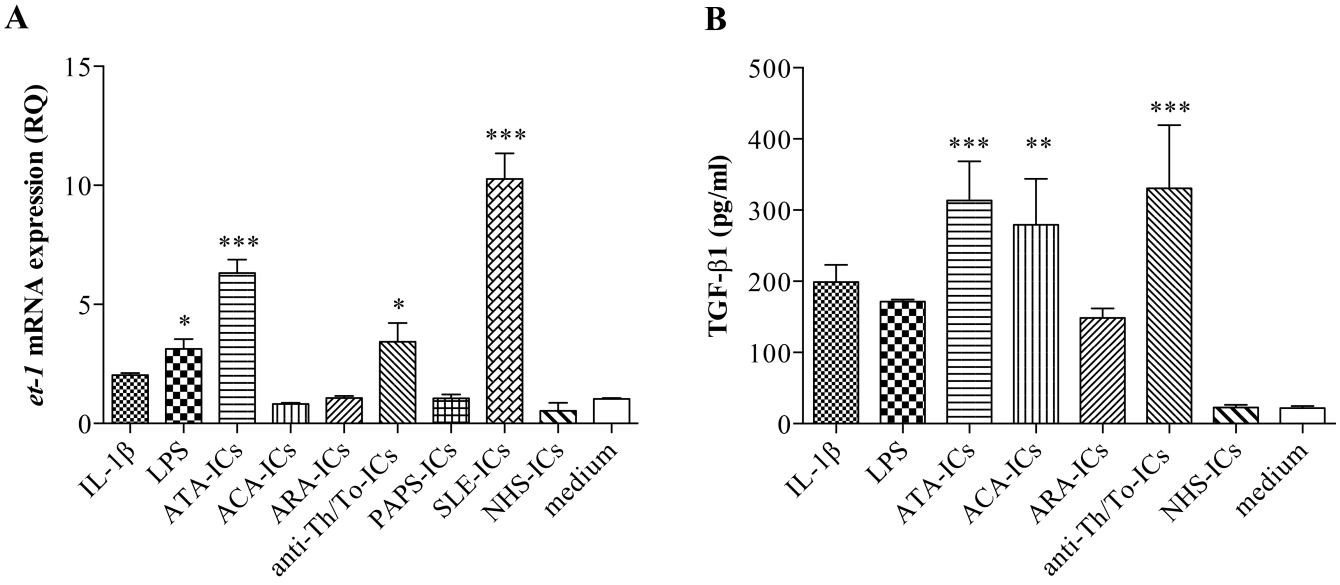

Figure 2

et-1 mRNA expression levels in HUVECs stimulated with SSc-ICs, PAPS-ICs, SLE-ICs and NHS-ICs; TGF-β1 secretion in HUVEC stimulated with SSc-ICs or NHS-ICs. Endothelial cells were incubated with SSc-ICs, PAPS-ICs, SLE-ICs or NHS-ICs (1:2 dilution). IL-1β (50 U/ml) and LPS (1 μg/ml) were used as positive controls. *p<0.01; **p<0.001; ***p<0.0001 versus medium. (A): et-1 (RQ) [mean±SD]. IL-1β [2.03±0.15] versus medium [1.03±0.06] (p=N.S.), versus NHS-ICs (p=N.S.). LPS [3.13±0.71] versus medium (p<0.01), versus NHS-ICs (p<0.001). ATA-ICs [6.32±0.99] versus medium (p<0.0001) and versus NHS-ICs [0.53±0.59] (p<0.0001). ACA-ICs [0.80±0.10] versus medium (p=N.S.), versus NHS-ICs (p=N.S.). ARA-ICs [1.07±0.15] versus medium (p=N.S.), versus NHS-ICs (p=N.S.). Anti-Th/To-ICs [3.43±1.37] versus medium (p<0.01), versus NHS-ICs (p<0.001). PAPS-ICs [1.06±0.27] versus medium (p=N.S.), versus NHS-ICs (p=N.S.). SLE-ICs [10.27±1.86] versus medium (p<0.0001), versus NHS-ICs (p<0.0001). NHS-ICs

[0.53±0.59] versus medium (p=N.S.). (B): TGF-β1 (pg/ml) [mean±SD]. IL-1β [198.8±48.71] versus medium [21.75±6.24] (p=N.S.), versus NHS-ICs (p=N.S.). LPS [171.5±5.8] versus medium (p=N.S.), versus NHS-ICs (p=N.S.). ATA-ICs [313.5±109.9] versus medium (p<0.0001) and versus NHS-ICs [22.75±7.59] (p<0.0001). ACA-ICs [279.5±129.0] versus medium (p<0.001), versus NHS-ICs (p<0.001). ARA-ICs [148.5±26.71] versus medium (p=N.S.), versus NHS-ICs (p=N.S.). Anti-Th/To-ICs [330.8±177.4] versus medium (p<0.0001), versus NHS-ICs (p<0.0001). NHS-ICs [22.75±7.59] versus medium (p=N.S.).

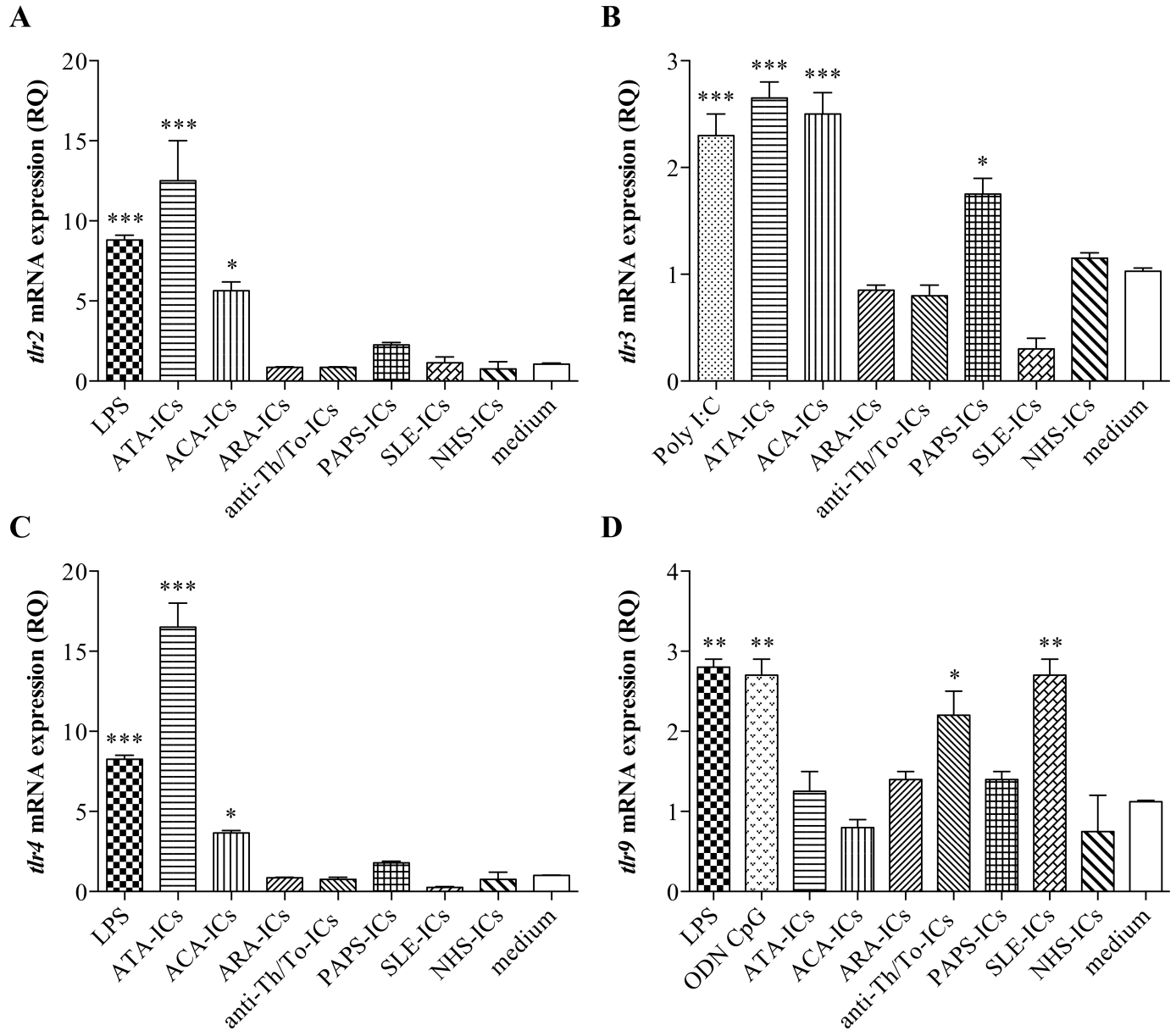

Figure 3

tlr mRNA expression levels in HUVECs stimulated with SSc-ICs, PAPS-ICs, SLE-ICs and NHS-ICs. Endothelial cells were incubated with SSc-ICs, PAPS-ICs, SLE-ICs or NHS-ICs (1:2 dilution). LPS (1 μg/ml), Poly I:C (1 μg/ml) and ODN CpG (5 μM) were used as positive controls. *p<0.01; **p<0.001; ***p<0.0001 versus medium. (A): tlr2 (RQ) [mean±SD]. LPS [8.8±0.42] versus medium [1.06±0.08] (p<0.0001), versus NHS-ICs (p<0.0001). ATA-ICs [12.50±3.54] versus medium (p<0.0001) and versus NHS-ICs [0.75±0.63]

(p<0.0001). ACA-ICs [5.65±0.78] versus medium (p<0.01), versus NHS-ICs (p<0.01). ARA-ICs [0.83±0.09] versus medium (p=N.S.), versus NHS-ICs (p=N.S.). Anti-Th/To-ICs [0.85±0.23] versus medium (p=N.S.), versus NHS-ICs (p=N.S.). PAPS-ICs [2.25±0.21] versus medium (p=N.S.), versus NHS-ICs (p=N.S.). SLE-ICs [1.15±0.49] versus medium (p=N.S.), versus NHS-ICs (p=N.S.). NHS-ICs [0.75±0.63] versus medium (p=N.S.). (B): tlr3 (RQ) [mean±SD]. Poly I:C [2.30±0.28] versus medium [1.03±0.04] (p<0.0001), versus NHS-ICs (p<0.0001). ATA-ICs [2.65±0.21] versus medium (p<0.0001) and versus NHS-ICs [1.15±0.07] (p<0.0001). ACA-ICs [2.5±0.28] versus medium (p<0.0001), versus NHS-ICs (p<0.0001). ARA-ICs [0.85±0.07] versus medium (p=N.S.), versus NHS-ICs (p=N.S.). Anti-Th/To-ICs [0.80±1.14] versus medium (p=N.S.), versus NHS-ICs (p=N.S.). PAPS-ICs [1.75±0.21] versus medium (p<0.01), versus NHS-ICs (p<0.01). SLE-ICs [0.30±0.14] versus medium (p<0.01), versus NHS-ICs (p<0.001). NHS-ICs [1.15±0.07] versus medium (p=N.S.). (C): tlr4 (RQ) [mean±SD]. LPS [8.25±0.35] versus medium [1.01±0.02] (p<0.0001), versus NHS-ICs (p<0.0001). ATA-ICs [16.50±2.12] versus medium (p<0.0001) and versus NHS-ICs [1.15±0.07] (p<0.0001). ACA-ICs [3.65±0.21] versus medium (p<0.01), versus NHS-ICs (p<0.0001). ARA-ICs [0.80±0.14] versus medium (p=N.S.), versus NHS-ICs (p<0.01). Anti-Th/To-ICs [0.70±0.28] versus medium (p=N.S.), versus NHS-ICs (p=N.S.). PAPS-ICs [1.85±0.21] versus medium (p=N.S.), versus NHS-ICs (p=N.S.). SLE-ICs [0.35±0.17] versus medium (p=N.S.), versus NHS-ICs (p=N.S.). NHS-ICs [1.21±0.57] versus medium (p=N.S.). (D): tlr9 (RQ) [mean±SD]. LPS [2.8±0.14] versus medium [1.12±0.03] (p<0.001), versus NHS-ICs (p<0.0001). ODNCpG [2.7±0.28] versus medium (p<0.001), versus NHS-ICs (p<0.0001). ATA-ICs [1.25±0.35] versus medium (p=N.S.) and versus NHS-ICs [0.75±0.64] (p=N.S.). ACA-ICs [0.9±0.2] versus medium (p=N.S.), versus NHS-ICs (p=N.S.).. ARA-ICs [1.4±0.13] versus medium (p=N.S.), versus NHS-ICs (p=N.S.). Anti-Th/To-ICs [2.20±0.42] versus medium (p<0.01), versus NHS-ICs (p<0.001). PAPS-ICs [1.4±0.12] versus medium (p=N.S.), versus NHS-ICs (p=N.S.). SLE-ICs [2.70±0.28] versus medium (p<0.001), versus NHS-ICs (p<0.0001). NHS-ICs [0.85±0.49] versus medium (p=N.S.).

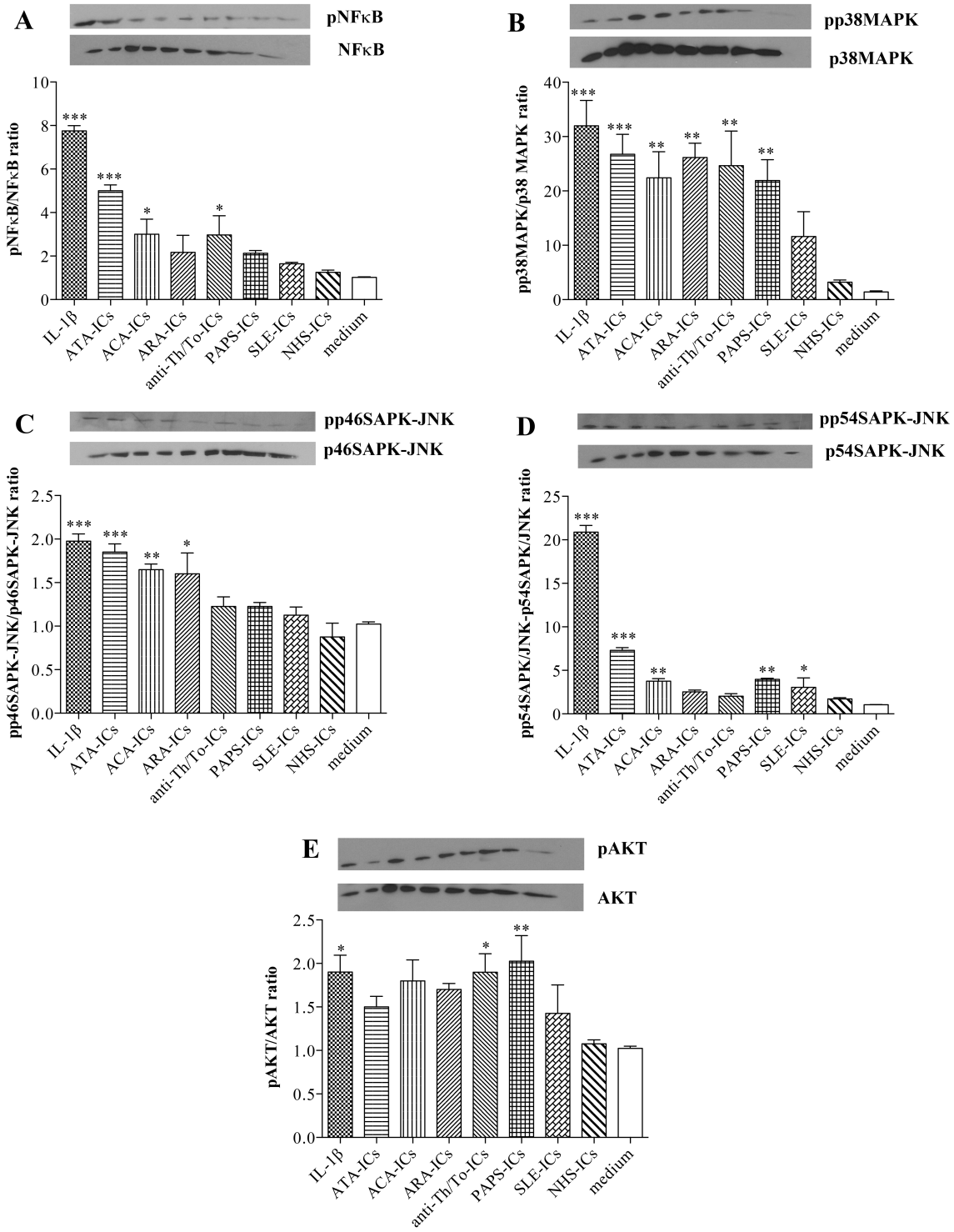

Figure 4

Intra-cellular signaling pathways in HUVECs stimulated with SSc-ICs, PAPS-ICs, SLE-ICs or NHS-ICs. Endothelial cells were incubated with SSc-ICs, PAPS-ICs, SLE-ICs or NHS-ICs (1:2 dilution). IL-1□□(50 U/ml) was used as positive control. Results are expressed as the ratio of phosphorylated to non-phosphorylated forms, evaluated using Image J software. Western Blotting images are representative of a single experiment. pNF□B: phosphorylated NF□B; p38MAPK: phosphorylated p38MAPK; pp46SAPK-JNK:

phosphorylated p46SAPK-JNK; pp54SAPK-JNK: phosphorylated p54SAPK-JNK; pAKT: phosphorylated AKT. Histograms represent mean ± standard error of the mean (SEM). *p<0.01; **p<0.001; ***p<0.0001 versus medium. (A): pNF□B/NFkB. IL-1□ [7.75±0.49] versus medium [1.02±0.05] (p<0.0001), versus NHS-ICs (p<0.0001). ATA-ICs [5.00±0.55] versus medium (p<0.0001) and versus NHS-ICs [22.75±7.59] (p<0.0001). ACA-ICs [3.00±1.39] versus medium (p<0.01), versus NHS-ICs (p=N.S.). ARA-ICs [2.17±1.55] versus medium (p=N.S.), versus NHS-ICs (p=N.S.). Anti-Th/To-ICs [2.98±1.75] versus medium (p<0.01), versus NHS-ICs (p=N.S.). PAPS-ICs [2.13±0.26] versus medium (p=N.S.), versus NHS-ICs (p=N.S.). SLE-ICs [1.65±0.13] versus medium (p=N.S.), versus NHS-ICs (p=N.S.). NHS-ICs [1.25±0.21] versus medium (p=N.S.). (B): pp38/p38. IL-1□ [31.98±9.37] versus medium [1.4±0.4] (p<0.0001), versus NHS-ICs (p<0.0001). ATA-ICs [26.75±7.3] versus medium (p<0.0001) and versus NHS-ICs [22.75±7.59] (p<0.001). ACA-ICs [22.43±9.57] versus medium (p<0.001), versus NHS-ICs (p<0.01). ARA-ICs [26.15±5.27] versus medium (p<0.001), versus NHS-ICs (p<0.001). Anti-Th/To-ICs [24.65±12.77] versus medium (p<0.001), versus NHS-ICs (p<0.001). PAPS-ICs [21.93±7.77] versus medium (p<0.001), versus NHS-ICs (p<0.01). SLE-ICs [11.63±9.14] versus medium (p=N.S.), versus NHS-ICs (p=N.S.). NHS-ICs [3.2±0.85] versus medium (p=N.S.). (C): pp46SAPK-JNK/p46SAPK-JNK. IL-1□ [1.98±0.17] versus medium [1.03±0.05] (p<0.0001), versus NHS-ICs (p<0.0001). ATA-ICs [1.85±0.19] versus medium (p<0.0001) and versus NHS-ICs [22.75±7.59] (p<0.0001). ACA-ICs [1.65±0.13] versus medium (p<0.001), versus NHS-ICs (p<0.0001). ARA-ICs [1.60±0.48] versus medium (p<0.01), versus NHS-ICs (p<0.001). Anti-Th/To-ICs [1.23±0.22] versus medium (p=N.S.), versus NHS-ICs (p=N.S.). PAPS-ICs [1.22±0.09] versus medium (p=N.S.), versus NHS-ICs (p=N.S.). SLE-ICs [1.13±0.19] versus medium (p=N.S.), versus NHS-ICs (p=N.S.). NHS-ICs [0.88±0.32] versus medium (p=N.S.). (D): pp54SAPK-JNK/p54SAPK-JNK. IL-1□ [20.88±1.56] versus medium [1.05±0.06] (p<0.0001), versus NHS-ICs (p<0.0001). ATA-ICs [7.30±0.63] versus medium [21.75±6.24] (p<0.0001) and versus NHS-ICs [22.75±7.59] (p<0.0001). ACA-ICs [3.75±0.59] versus medium (p<0.001), versus NHS-ICs (p<0.01). ARA-ICs [2.52±0.41] versus medium (p=N.S.), versus NHS-ICs (p=N.S.). Anti-Th/To-ICs [2.02±0.60] versus medium (p=N.S.), versus NHS-ICs (p=N.S.). PAPS-ICs [3.98±0.24] versus medium (p<0.001), versus NHS-ICs (p<0.01). SLE-ICs [3.05±2.17] versus medium (p<0.01), versus NHS-ICs (p=N.S.). NHS-ICs [1.73±0.28] versus medium (p=N.S.). (E): pAKT/AKT. IL-1□ [1.90±0.39] versus medium [1.02±0.05] (p<0.01), versus NHS-ICs (p<0.01). ATA-ICs [1.50±0.24] versus medium [21.75±6.24] (p=N.S.) and versus NHS-ICs [22.75±7.59] (p=N.S.). ACA-ICs [1.80±0.48] versus medium (p=N.S.), versus NHS-ICs (p=N.S.). ARA-ICs [1.70±0.14] versus medium (p=N.S.), versus NHS-ICs (p=N.S.). Anti-Th/To-ICs [1.90±0.42] versus medium (p<0.01), versus NHS-ICs (p<0.01). PAPS-ICs [2.02±0.59] versus medium (p<0.001), versus NHS-ICs (p<0.01). SLE-ICs [1.42±0.65] versus medium (p=N.S.), versus NHS-ICs (p=N.S.). NHS-ICs [1.08±0.10] versus medium (p=N.S.).

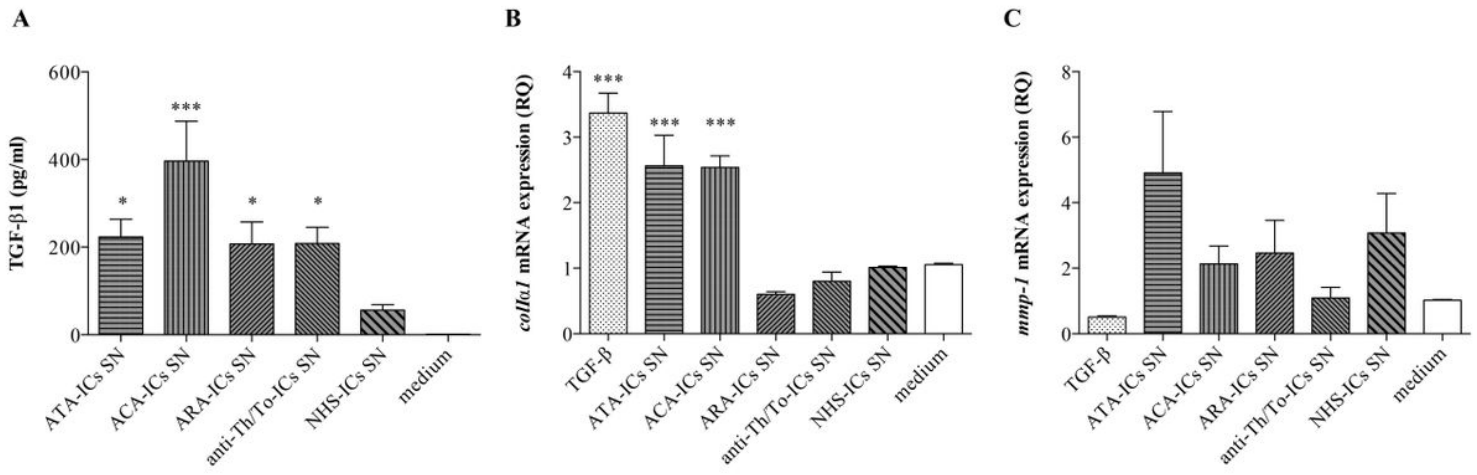

Figure 5

TGF-β1 secretion and collα1 and mmp-1 mRNA expression in fibroblasts stimulated with supernatants from HUVEC incubated with SSc-ICs or NHS-ICs. Fibroblasts were exposed to supernatants from HUVECs incubated with SSc-ICs or NHS-ICs (1:2 dilution). TGF-β1 (10 ng/ml) was used as positive control for collagen and mmp-1 synthesis. Histograms represent mean ± standard error of the mean (SEM). *p<0.01; ***p<0.0001 versus medium. (A): TGF-β1 (pg/mL) (mean±SD). ATA-ICs [223.2±90.60] versus medium [1.08±0.22] (p<0.01) and versus NHS-ICs [56.25±24.92] (p=N.S.). ACA-ICs [396.20±203.90] versus medium (p<0.0001), versus NHS-ICs (p<0.0001). ARA-ICs [207.40±111.70] versus medium (p<0.01), versus NHS-ICs (p=N.S.). Anti-Th/To-ICs [208.40±97.70] versus medium (p<0.01), versus NHS-ICs (p=N.S.). NHS-ICs [56.25±24.92] versus medium (p=N.S.). (B): collα1 (RQ) [mean±SD]. TGF-β [3.37±0.42] versus medium [1.05±0.04] (p<0.0001), versus NHS-ICs (p<0.0001). ATA-ICs [2.56±0.93] versus medium (p<0.0001) and versus NHS-ICs [1±0.5] (p<0.0001). ACA-ICs [2.54±0.35] versus medium (p<0.0001), versus NHS-ICs (p<0.0001). ARA-ICs [0.60±0.08] versus medium (p=N.S.), versus NHS-ICs (p=N.S.). Anti-Th/To-ICs [0.80±0.28] versus medium (p=N.S.), versus NHS-ICs (p=N.S.). NHS-ICs [1±0.4] versus medium (p=N.S.). (C): mmp-1 (RQ) [mean±SD]. TGF-β [0.51±0.04] versus medium [1.02±0.04] (p=N.S.), versus NHS-ICs (p=N.S.). ATA-ICs [4.91±3.74] versus medium (p=N.S.) and versus NHS-ICs [3.08±2.40] (p=N.S.). ACA-ICs [0.13±1.09] versus medium (p=N.S.), versus NHS-ICs (p=N.S.). ARA-ICs [2.46±2.0] versus medium (p=N.S.), versus NHS-ICs (p=N.S.). Anti-Th/To-ICs [1.09±0.65] versus medium (p=N.S.), versus NHS-ICs (p=N.S.). NHS-ICs [3.08±2.40] versus medium (p=N.S.).

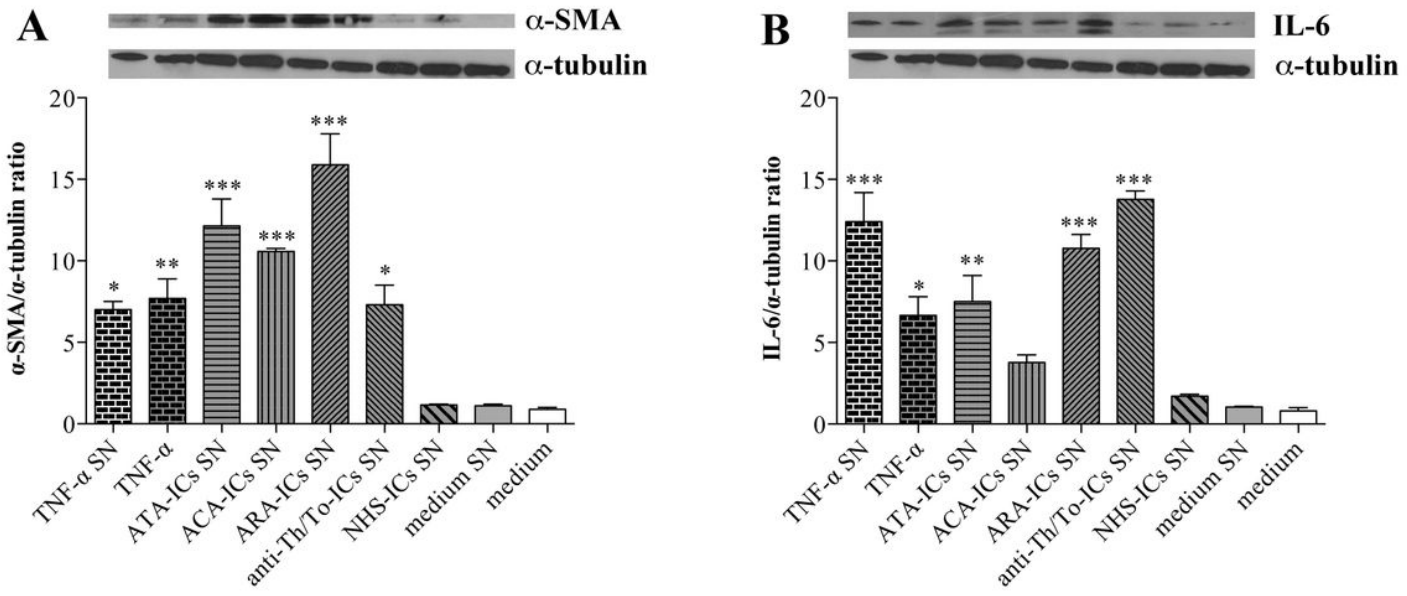

Figure 6

□□SMA and IL-6 protein expression in fibroblasts stimulated with supernatants from HUVEC incubated with SSc-ICs and NHS-ICs. Fibroblasts were exposed to supernatants from HUVECs incubated with TNF-□ (10 ng/mL), SSc-ICs or NHS-ICs (1:2 dilution). TNF-□ (10 ng/mL) was used as positive control. SN: supernatants. Histograms represent mean ± standard error of the mean (SEM). *p<0.01; ***p<0.0001 versus medium. (A) □□SMA. TNF-□ SN [7.0±0.71] versus medium SN [1.1±0.14] (p<0.01), versus NHS-ICs SN (p<0.01). TNF-□ [7.70±1.70] versus medium [0.9±0.15] (p<0.001). ATA-ICs SN [12.15±2.33] versus medium SN (p<0.0001) and versus NHS-ICs SN [1.15±0.07] (p<0.0001). ACA-ICs SN [10.58±0.25] versus medium SN (p<0.0001), versus NHS-ICs SN (p<0.0001). ARA-ICs SN [15.90±2.70] versus medium SN (p<0.0001), versus NHS-ICs SN (p<0.0001). Anti-Th/To-ICs SN [7.30±1.69] versus medium SN (p<0.01), versus NHS-ICs SN (p<0.01). NHS-ICs SN [1.15±0.07] versus medium SN (p=N.S.). (B) IL-6. TNF-□ SN [12.41±2.54] versus medium SN [1.05±0.07] (p<0.0001), versus NHS-ICs SN (p<0.0001). TNF-□ [6.65±1.63] versus medium [0.08±0.28] (p<0.01). ATA-ICs SN [7.50±2.26] versus medium SN (p<0.001) and versus NHS-ICs SN [1.71±0.17] (p<0.01). ACA-ICs SN [3.77±0.66] versus medium SN (p=N.S.), versus NHS-ICs SN (p=N.S.). ARA-ICs SN [10.77±1.22] versus medium SN (p<0.0001), versus NHS-ICs SN (p<0.0001). Anti-Th/To-ICs SN [13.78±0.73] versus medium SN (p<0.0001), versus NHS-ICs SN(p<0.0001). NHS-ICs SN [1.71±0.17] versus medium SN (p=N.S.).